Designer Spin Pseudomolecule Implemented with Trapped Ions in a Magnetic Gradient

A. Khromova, Ch. Piltz, B. Scharfenberger, T. F. Gloger, M. Johanning, A. F. Varón, and Ch. Wunderlich*
Department Physik, Naturwissenschaftlich-Technische Fakultät, Universität Siegen, 57068 Siegen, Germany
(Dated: 11 November 2011)

We report on the experimental investigation of an individual pseudomolecule using trapped ions with adjustable magnetically induced J-type coupling between spin states. Resonances of individual spins are well separated and are addressed with high fidelity. Quantum gates are carried out using microwave radiation in the presence of thermal excitation of the pseudomolecule's vibrations. Demonstrating Controlled-NOT gates between non-nearest neighbors serves as a proof-of-principle of a quantum bus employing a spin chain. Combining advantageous features of nuclear magnetic resonance experiments and trapped ions, respectively, opens up a new avenue towards scalable quantum information processing.

PACS numbers: 03.67.Lx 03.65.Ud 37.10.Ty 42.50.Dv

Successful experiments with molecules using nuclear magnetic resonance (NMR) [1–7] and with trapped ions [8–12] have been an important driving force for quantum information science. Early on during the development of quantum information science NMR was successfully applied to carry out sophisticated quantum logic operations and complete quantum algorithms based on the so-called J-coupling between nuclear spins in molecules. In molecules used for NMR, the direct dipole-dipole interaction between nuclear spins is usually negligible. However, nuclear spins interact indirectly via J-coupling which is mediated by bonding electrons. This J-coupling provides a mechanism to implement conditional quantum dynamics with nuclear spins that are characterized by long coherence times and are manipulated using rf radiation. Scalability of NMR is hampered mainly by the use of ensembles of molecules making it difficult to prepare pure spin states. Also, nuclear spin resonances and J-coupling between spins in molecules are given by nature, and thus often are not well suited for quantum computing.

Here, effective spin-1/2 systems are realized by using long-lived hyperfine states of trapped atomic ions. The vibrational modes of this individual ion pseudomolecule [13] mediate an effective J-type coupling when exposing trapped ions to a spatially varying magnetic field [14–16]. The constants J_{ij} arising from magnetic gradient induced coupling (MAGIC) of such an individual spin-pseudo-molecule can be adjusted through variation of the trapping potential that determines the frequencies ν_n of the ion crystal's vibrational modes. In addition, the range of interactions can be tuned by applying local static potentials [16, 17]. Single spins can be addressed in frequency space, since the magnetic field gradient leads to a position dependent shift of an ion's resonance frequency [18, 19]. A further useful feature of spin-pseudomolecules is the use of radio-frequency and microwave radiation for conditional quantum dynamics as opposed to laser light [18–21], a feature that substantially reduces experimental complexity and contributed to the rapid success of NMR in quantum information science. In addition, this eliminates spontaneous emission that otherwise may destroy coherences [22]. Moreover, J-type coupling in a spin-pseudomolecule is tolerant against thermal excitation of vibrational motion. This substantially reduces the necessity for cooling trapped ions in order to achieve high fidelity gates.

Exposing a trapped ion Coulomb crystal to a spatially varying magnetic field induces a spin-spin interaction mediated by the common vibrational motion of the ion crystal [14, 15],

$$H = -\frac{\hbar}{2}\sum_{i<j}^{N} J_{ij}\sigma_z^{(i)}\sigma_z^{(j)}, \tag{1}$$

where σ_z is a Pauli matrix and the coupling constants $J_{ij} = \sum_{n=1}^{N} \nu_n \kappa_{ni}\kappa_{nj}$. This sum extends over all vibrational modes with angular frequency ν_n, and $\kappa_{nl} \equiv \frac{\Delta z \partial_z \omega_l}{\nu_n} S_{nl}$ indicates how strongly ion l couples to the vibrational mode n, when the spin of ion l is flipped. Here, $\Delta z = \sqrt{\hbar/2m\nu_n}$ is the extension of the ground state wave function of vibrational mode n, and $\Delta z \partial_z \omega_l = g_F \mu_B b_l/\hbar$ gives the change of the ion's resonance frequency ω_l when moving it by Δz (b_l is the magnetic field gradient at the position of ion l, $\hbar$ is the reduced Planck's constant, μ_B the Bohr magneton, and g_F the Landé factor, *e.g.*, $g_F = 1$ for $^{171}Yb^+$ ions in the electronic ground state). The dimensionless matrix elements S_{nl} give the scaled deviation of ion l from its equilibrium positions when vibrational mode n is excited. Such magnetic gradient induced coupling may also be implemented using electrons confined in a Penning trap [23]. Tunable spin-spin coupling based on optical dipole forces was proposed in [24] and demonstrated in [25, 26].

After outlining how individual spins can be addressed with high fidelity in what follows, the measurement of the coupling matrix $\{J_{ij}\}$ for a three-spin-pseudomolecule is described. In addition, it is shown how coupling constants can be adjusted by variation of

the ion trapping potential. Then, the experimental realization of controlled-NOT gates between any pair of spins is described, including a CNOT gate between non-neighboring ions. The entanglement of spins is proven by measuring the parity (defined below) of a two-spin state.

Hyperfine levels of the $^2S_{1/2}$ ground state of $^{171}Yb^+$ serve as an effective spin-1/2 system [15], namely $|\downarrow_i\rangle \equiv {}^2S_{1/2}$ (F=0) and $|\uparrow_i\rangle \equiv {}^2S_{1/2}$ (F=1, $m_F = +1$), where $i = 1, 2, 3$ refers to ion i. These states are coherently controlled by microwave radiation near 12.65 GHz in resonance with the $|\downarrow_i\rangle \leftrightarrow |\uparrow_i\rangle$ transition. For the experiments presented here we load three $^{171}Yb^+$ ions in a linear Paul trap where the effective harmonic trapping potential is characterized by the secular radial frequency $\nu_r = 2\pi \times 502(2)$ kHz and axial frequency $\nu_1 = 2\pi \times 123.5(2)$ kHz. Initial preparation in state $|\downarrow\rangle$ is achieved by optical pumping on the $^2S_{1/2}$ (F=1) $\leftrightarrow$ $^2P_{1/2}$ (F=1) transition near 369 nm, and state-selective detection is done by registering resonance fluorescence scattered on the $^2S_{1/2}$ (F=1) $\leftrightarrow$ $^2P_{1/2}$ (F=0) electronic transition. This ionic resonance serves at the same time for Doppler cooling of the ion crystal. The population of the center-of-mass (c.m.) mode after Doppler cooling along the axial direction is $\langle n_1 \rangle \approx 150$. Microwave sideband cooling is applied to attain $\langle n_1 \rangle = 23(7)$ (details will be published elsewhere).

The ions are exposed to a magnetic field gradient along the z direction that is created by two hollow cylindrical SmCo permanent magnets plated with nickel and mounted at each end-cap electrode of the trap with identical poles facing each other. The total magnetic field amplitude is given by $B(z) = \sqrt{(B_{0||} + b_{\rm pm} z)^2 + B_{0\perp}^2}$, where $B_{0||} = 3.4 \times 10^{-4}$ T and $B_{0\perp} = 6.2 \times 10^{-5}$ T are longitudinal and radial components of the bias field at the coordinate origin defined by the position of the center ion, and $b_{\rm pm}$=19.0(1) T/m is the magnetic field gradient created by the permanent magnets in the absence of a perpendicular bias field. The magnetic field gradient $b_l = \partial_z B(z)|_{z=z_l}$ defined at the position z_l of ion l is smaller than $b_{\rm pm}$ and not constant due to the nonzero radial component $B_{0\perp}$ of the bias field.

The state $|\uparrow\rangle$ is magnetically sensitive and undergoes an energy shift $\Delta E = g_F \mu_B B$ due to the linear Zeeman effect, while state $|\downarrow\rangle$ to first order is insensitive to the magnetic field. Because to the gradient of the magnetic field, three ions with an inter-ion spacing of 11.9 μm [Fig. 1(a)] are subject to different energy shifts resulting in a frequency shift of the resonance $|\downarrow\rangle \leftrightarrow |\uparrow\rangle$ of approximately $\Delta f \simeq 3$ MHz between adjacent ions [Fig. 1(b)]. This energy shift makes it possible to address independently the ions in frequency space by using microwave radiation (or laser light [27]). The probability amplitude of exciting a neighboring ion decreases with the square of the detuning. Here, it is less than 4×10^{-4} (see Supplemental Material [28]).

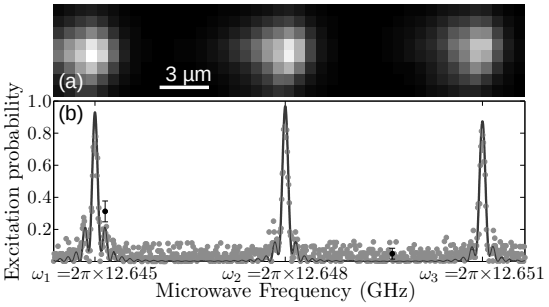

FIG. 1. Individual addressing of spins. (a) Spatially resolved resonance fluorescence (near 369 nm) of three ^{171}Yb$^+$ions recorded with an intensified CCD camera is shown. Neighboring ions are separated by 11.9 μm. (b) Microwave-optical double resonance spectrum of the above ions. The spectrum was recorded by applying a microwave frequency pulse of 8 μs to the ions initially prepared in the state $|\downarrow\rangle$. The probability to find an ion in $|\uparrow\rangle$ was determined from counting resonance fluorescence photons while probing with laser light near 369 nm. In a magnetic gradient of ≈ 18.2 T/m, the qubit transitions $|\downarrow\rangle \leftrightarrow |\uparrow\rangle$ of different ions are nondegenerate. The solid line is a fit to the data. Each data point accounts for 50 repetitions. Two points with error bars are displayed representing the typical statistical standard deviations.

In addition, the magnetic gradient induces the spin-spin interaction Eq. (1) between the ions' internal states mediated by their common vibrational modes. Not only nearest neighbors interact but also the outer ions 1 and 3. The coupling constants J_{12}, J_{23} and J_{13} have been measured in a Ramsey-type experiment and are displayed in Fig. 2(a) together with their calculated values. For these measurements, first all three ions are initialized in state $|\downarrow\downarrow\downarrow\rangle$. After a microwave $\pi/2$ pulse has been applied to ion j, this spin's precession will depend on the state of ion i which can be left in state $|\downarrow_i\rangle$ or set to $|\uparrow_i\rangle$ by a microwave π pulse. After time τ, a second $\pi/2$ pulse with variable phase ϕ is applied and the population $P(\phi)$ of $|\uparrow_j\rangle$ is measured with ion i initially prepared in state $|\downarrow_i\rangle$ or in $|\uparrow_i\rangle$, respectively. The coupling between ions i and j is then deduced from the phase difference $\Delta\phi_{ij}$ between these two sinusoidal signals $P(\phi)$: $J_{ij} = \Delta\phi_{ij}/2\tau$. In order to extend the coherence time of the spin states, which is limited by ambient magnetic field fluctuations, a multi pulse spin-echo sequence is applied to ions i and j between the $\pi/2$-Ramsey pulses [28]. The third ion (labeled k) has no active role and is left in state $|\downarrow_k\rangle$ during the whole sequence. Its interaction with the other ions via J-coupling is cancelled by the applied spin-echo sequence (which is true independent of its internal state).

It is possible to encode quantum information in two sets of states, where one set is magnetically sensitive (as

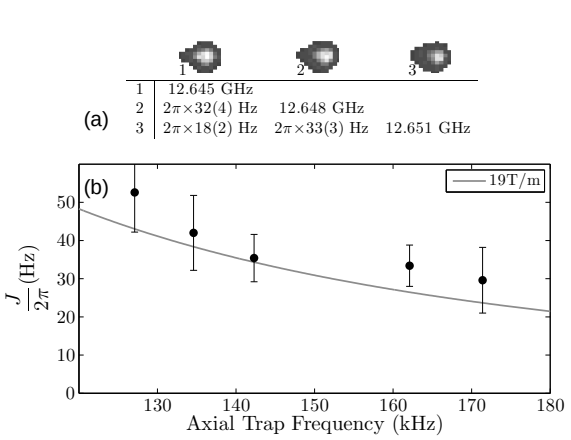

FIG. 2. J-type coupling of a three-spin pseudomolecule. In (a), the table lists the measured J-type coupling constants (below the diagonal) for a three-spin pseudomolecule together with the resonance frequencies of the microwave transitions (on the diagonal). For the nonuniform magnetic gradient present in our setup ($b_1 = 16.8$ T/m, $b_2 = 18.7$ T/m, $b_3 = 18.9$ T/m) and the axial trap frequency ($\nu_1 = 2\pi \times 123.5$ kHz) the calculated values are $J_{12} = 2\pi \times 32.9$ Hz, $J_{23} = 2\pi \times 37.0$ Hz, $J_{13} = 2\pi \times 23.9$ Hz.
(b) Dependence of the coupling strength on the trapping potential. For a pseudo-molecule consisting of two ions, the coupling strength J has been measured for varying c. m. frequency ν_1. A calculated curve for a uniform magnetic gradient of 19 T/m is represented by a solid line. These measurements demonstrate how J-type coupling can be varied by adjusting the trapping potential [16, 17].

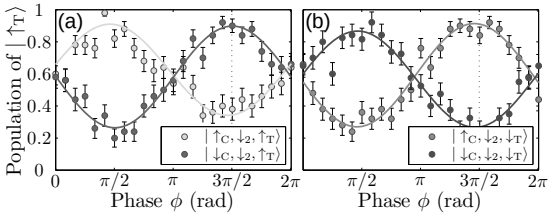

FIG. 3. Conditional quantum dynamics and CNOT gate between non-neighboring ions. The probability to find the target spin (ion 3) in state $|\uparrow\rangle$ at the end of a Ramsey-type sequence is shown as a function of the phase ϕ of the second $\pi/2$ pulse applied to the target. The inset shows the input state prepared before the Ramsey experiment. In a) the target is initially prepared in $|\uparrow\rangle$ while in b) it is prepared in $|\downarrow\rangle$. J-type coupling between the control qubit (ion 1) and the target qubit (ion 3) produces a phase shift on the target population as a function of the control qubit's state (different shades of gray). A free evolution time of $\tau = 11$ ms yields a phase shift of approximately π (3.1(2) radians) between the pairwise displayed curves. For $\phi = 3\pi/2$, a CNOT gate results. The middle ion, prepared in state $|\downarrow\rangle$, does not interact with other ions. Each data point represents 50 repetitions, the error bars correspond to mean standard deviations and solid lines are fits to the data.

is used in this work), and the other set is not [e.g., $^2S_{1/2}$ (F=1, $m_F = 0$) and ($F = 0$)]. This allows for temporal storage of quantum information in magnetically insensitive states that do not couple to other spins and provide a memory intrinsically robust against ambient field fluctuations.

Figure 2(b) shows the dependence of J-type coupling on the c.m. frequency ν_1, that is, on the strength of the axial trapping potential. These data were taken with two trapped ions with the measurements carried out analogous to those described above, except that only a single spin-echo pulse was used here. This leads to shorter accessible precession times and thus smaller phase shifts which in turn yields a larger statistical error as compared to the data in Fig. 2(a). The data are in agreement with the calculated dependence of J on ν_1 ($J \propto (b/\nu_1)^2$).

J-type coupling between two spins is employed to implement a CNOT gate between ion 1 (control qubit) and ion 3 (target qubit). The evolution time $\tau = 11$ ms is chosen to achieve a phase shift of $\Delta\phi_{13} = \pi$. Figures 3(a) and (b) show the resulting state population of the target qubit as a function of phase ϕ of the last $\pi/2$-Ramsey pulse which is applied to the target qubit. The CNOT operation is achieved when selecting $\phi = 3\pi/2$. The four measured sets of data are in agreement with the truth table of the CNOT gate which induces a flip of the target qubit or leaves it unchanged depending on the initial state $|\uparrow\rangle$ or $|\downarrow\rangle$ of the control qubit.

The quantum nature of the conditional gate is verified by creation of entanglement in the outcome $|\psi_B\rangle = \frac{1}{\sqrt{2}}(|\downarrow_C\downarrow_2\downarrow_T\rangle + \mathrm{e}^{i\alpha}\,|\uparrow_C\downarrow_2\uparrow_T\rangle)$ if the input is a superposition state. Only the correlations of the control and target qubit determine the parity $\Pi = P_{\uparrow\uparrow} + P_{\downarrow\downarrow} - (P_{\uparrow\downarrow} + P_{\downarrow\uparrow})$ of the resulting bipartite entangled Bell state ($P_{ij},\ i,j = \downarrow,\uparrow$ denotes the probability to find the control and target qubits in the state $|ij\rangle$). When measuring in the σ_z basis, we observe a parity $\Pi_z = 0.43(13)$. To prove that the correlations are nonclassical, the parity $\Pi(\phi)$ was measured in addition along different bases [10] by applying additional $\pi/2$ pulses with phase ϕ to both ions. Figure 4 shows the resulting signal $\Pi(\phi)$ that oscillates with twice the phase variation, as one would expect for a bipartite entangled state. From the visibility of $V = 0.42(6)$ of the signal shown in Fig. 4 we evaluate the fidelity [10] of a Bell state $F = \frac{\Pi_z+1}{4} + \frac{V}{2}$ to be 0.57(4) which exceeds the Bell limit of 0.5 and thus proves the existence of entanglement. This shows that a conditional quantum gate between two non-neighboring ions is achieved.

In a similar manner, a CNOT gate was achieved between the first and the second ion with a fidelity of $F = 0.64(5)$ showing that it is possible to carry out on demand entangling operations between two ions at de-

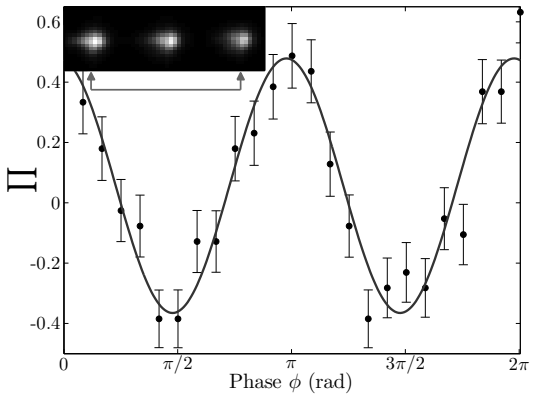

FIG. 4. Parity signal $\Pi(\phi)$ showing the quantum nature of the observed correlations of ion 1 and 3. The Bell state $|\psi_B\rangle = \frac{1}{\sqrt{2}}(|\downarrow_C\downarrow_2\downarrow_T\rangle + \mathrm{e}^{i\alpha}\,|\uparrow_C\downarrow_2\uparrow_T\rangle)$ is the result of a CNOT operation applied to the superposition input state $|\psi_i\rangle = \frac{1}{\sqrt{2}}(|\downarrow_C\downarrow_2\downarrow_T\rangle + |\uparrow_C\downarrow_2\downarrow_T\rangle)$. In order to measure the correlations along different bases [10], microwave $\pi/2$-pulses with phase ϕ are applied to both ions followed by state-selective detection resulting in $\Pi(\phi)$ oscillating as $\cos(2\phi)$. The fidelity of creating the bipartite entangled state $|\psi_B\rangle$ is evaluated as $F = 0.57(4)$ (see text). Each data point represents 50 repetitions and error bars indicate 1 standard deviation.

sired positions of the ion chain. For neighboring ions the coupling constants are higher allowing for shorter evolution times (in this case 8 ms) and therefore reducing the effect of decoherence. In future experiments, microwave dressed states will be employed to extend the coherence time of magnetic sensitive states by several orders of magnitude [21], and thus the fidelity of quantum gates will be improved.

The entanglement procedure shown here can be applied to longer ion chains with minimal modifications. A large-scale quantum processor would be made up of an array of traps [11] each containing a spin-pseudomolecule allowing for simultaneous conditional quantum dynamics with more than two spins (multiqubit gates). This could substantially speed up the execution of quantum algorithms [29] and would be an alternative to a processor that contains zones for conditional quantum dynamics with two or three ions [11]. Importantly, physical relocation ("shuttling") of ions could be avoided during the processing of quantum information within a given spin-pseudomolecule [29]. The possibility to directly perform logic gates between distant qubits (e.g., the endpoints of a spin chain as demonstrated here) makes spin-pseudomolecules suitable as a quantum bus connecting different processor regions [30]. In that case, shuttling would be restricted to a pair of messenger ions which enable communication between different spin-pseudomolecules. In addition, a spin-pseudomolecule could serve as a versatile tool for quantum simulations of otherwise intractable physical systems [24–26, 31, 32].

It is desirable to increase the J-type constants due to MAGIC. This will be attained in micro-structured ion traps [33, 34] and trap arrays that allow for the application of larger magnetic gradients, or by using magnetic field gradients oscillating near the trap frequency [35]. In addition, segmented traps will allow for shaping J-coupling matrices by applying local electrostatic potentials [16, 17], for example, to create cluster states [36], or to perform quantum simulations.

Assistance in data-taking by T. Collath and D. Kaufmann and discussions with O. Gühne are gratefully acknowledged, as well as financial support by the Bundesministerium für Bildung und Forschung (FK 01BQ1012), Deutsche Forschungsgemeinschaft, and the European Commission under STREP PICC and iQIT.

* wunderlich@physik.uni-siegen.de

[1] D. G. Cory, A. F. Fahmy, and T. F. Havel, Proc. Natl. Acad. Sci. U.S.A. **94**, 1634 (1997).
[2] I. L. Chuang *et al.*, Nature **393**, 143 (1998).
[3] J. A. Jones, M. Mosca, and R. H. Hansen, Nature **393**, 344 (1998).
[4] R. Marx *et al.*, Phys. Rev. A **62**, 012310 (2000).
[5] E. Knill, R. Laflamme, R. Martinez, and C. H. Tseng, Nature **404**, 368 (2000).
[6] L. M. K. Vandersypen, *et al.*, Nature **414**, 883 (2001).
[7] D. Suter and T. S. Mahesh, J. Chem. Phys. **128**, 052206 (2008).
[8] J. I. Cirac and P. Zoller, Phys. Rev. Lett. **74**, 4091 (1995).
[9] R. Blatt and D. Wineland, Nature **453**, 1008 (2008).
[10] C. A. Sackett, *et al.*, Nature **404**, 256 (2000).
[11] D. Kielpinski, C. Monroe, and D. J. Wineland, Nature **417**, 709 (2002).
[12] G. Kirchmair, *et al.*, New J. Phys. **11**, 023002 (2009).
[13] D. J. Wineland, *et al.*, Phys. Rev. Lett. **59**, 2935 (1987).
[14] Ch. Wunderlich, in *Laser Physics at the Limit*, edited by D. Meschede, C. Zimmermann, and H. Figger (Springer, New York, 2002) p. 261.
[15] Ch. Wunderlich, C. Balzer, in *Adv. At. Mol. Phys.* ***49***, edited by B. Benjamin, and W. Herbert, (Elsevier, London, 2003) p. 293.
[16] D. Mc Hugh and J. Twamley, Phys. Rev. A **71**, 012315 (2005).
[17] H. Wunderlich, Ch. Wunderlich, K. Singer, and F. Schmidt-Kaler, Phys. Rev. A **79**, 052324 (2009).
[18] F. Mintert and Ch. Wunderlich, Phys. Rev. Lett. **87**, 257904 (2001).
[19] M. Johanning, *et al.*, Phys. Rev. Lett. **102**, 073004 (2009).
[20] C. Ospelkaus, *et al.*, Nature **476**, 181 (2011).
[21] N. Timoney, *et al.*, Nature **476**, 185 (2011).
[22] N. Akerman, S. Kotler, Y. Glickman, and R. Ozeri, eprint arXiv:1111.1622v1 [quant-ph] (2011).
[23] G. Ciaramicoli, F. Galve, I. Marzoli, and P. Tombesi, Phys. Rev. A **72**, 042323 (2005).
[24] D. Porras and J. I. Cirac, Phys. Rev. Lett. **92**, 207901 (2004).
[25] A. Friedenauer, *et al.*, Nat. Phys. **4**, 757 (2008).

[26] K. Kim, *et al.*, Phys. Rev. Lett. **103**, 120502 (2009).
[27] S. X. Wang, J. Labaziewicz, Y. Ge, R. Shewmon, and I. L. Chuang, Appl. Phys. Lett. **94**, 094103 (2009).
[28] See Supplemental Material for information about the experiment and its imperfections that presently limit the fidelity of conditional quantum gates.
[29] T. Schulte-Herbrüggen, A. Spörl, N. Khaneja, and S. J. Glaser, Phys. Rev. A **72**, 042331 (2005).
[30] D. Gottesman and I. L. Chuang, Nature **402**, 390 (1999).
[31] Z. K. Li, *et al.*, Scientific Reports **1**: 88 (2011).
[32] P. A. Ivanov and F. Schmidt-Kaler, New J. Phys. **13**, 125008 (2011).
[33] M. D. Hughes, B. Lekitsch, J. A. Broersma, and W. K. Hensinger, Contemporary Physics **52**, 505 (2011).
[34] D. Kaufmann, *et al.*, *Appl. Phys. B: Lasers and Optics* in print, eprint arXiv:1107.4082v1 [quant-ph] (2012).
[35] J. Welzel, *et al.*, Eur. Phys. J. D **65**, 285 (2011).
[36] H. J. Briegel, *et al.*, Nat. Phys. **5**, 19 (2009).

SUPPLEMENTAL MATERIAL

In what follows the experimental pulse sequence used for the CNOT gate is explained. Imperfections that presently limit the fidelity of conditional quantum gates are also discussed.

CNOT Gate Pulse Sequence In order to extend the coherence time which in this experimental setup is currently limited to about 200 μs, a sequence of π-pulses sandwiched between the two $\pi/2$-Ramsey pulses is applied to both ions participating in the gate. This serves to refocus dephasing produced by ambient fluctuating fields. If these π-pulses were applied only to the target ion, they would not only refocus unwanted dephasing, but also the interaction with the control ion. Therefore, in order to keep the $J-$type interaction between the ions active (while compensating for errors caused by ambient fields) the control ion needs to be flipped each time the target ion is flipped, that is, the same sequence of π-pulses has to be applied simultaneously on both ions.

The sequence of π-pulses is a novel variant of the Carr-Purcell-Meiboom-Gill (CPMG) multipulse spin echo method [1]. Instead of using the original proposal of identical π-pulses, their relative phases were varied in order to obtain a self-correcting sequence that is only sparsely susceptible to experimental imperfections. Using a sequence with 84 pulses turned out to be a good compromise between suppressing decoherence and robustness. This sequence has also shown to be more robust than sequences based on uniform and alternating phases (details to be published elsewhere).

The sequence of pulses does not refocus magnetic field fluctuations on a timescale faster than τ. Therefore, for increased free evolution time a reduction of the contrast of the measured signals is observed (Fig. 3 of the paper). For a free evolution time of 11 ms, the decoherence accounts for a reduction of the final state fidelity of at least 30%. For an evolution time of 8 ms this reduction accounts for about 20% error. In future experiments microwave dressed states will be employed to extend the coherence time [2].

Addressing Errors While addressing one ion, it is possible to unintentionally change the state of a neighboring ion. The non-resonant excitation probability of neighboring ions is smaller than $\frac{\Omega^2}{\Omega^2+(g_F\mu_B bd/\hbar)^2}$ where Ω is the Rabi frequency, b the magnetic gradient and d the separation of two neighboring ions. In the case of an harmonic trap with axial confinement frequency ν_1 and N ions of mass m forming a linear chain, the biggest addressing errors arise in the middle of the chain where the ions are closest together. The minimum inter-ion spacing is given by $d_{min}(\nu_1, N) = \sqrt[3]{\frac{e^2}{4\pi\epsilon_0 m\nu_z^2}}\frac{2.018}{N^{0.559}}$, where e is the electron charge and ϵ_0 is the permittivity of free space [3]. In the experiments reported here, typically $\Omega \approx 2\pi \times 60$ kHz, $d \approx 12$ μm, and $b \approx 18$ T/m resulting in a spurious probability of less than 4×10^{-4}.

State Detection A photomultiplier is used to measure the parity signal shown in Fig. 4 of the paper. The number of photons detected is characterised by three Poissonian distributions that correspond to the number of ions (between zero and two) to be found in state $|\uparrow\rangle$.

In 98.5 % of the cases the correct state is detected when both ions are in $|\downarrow\rangle$ (no fluorescence ideally), 88.9% of the cases are detected correctly when one ion is in $|\uparrow\rangle$ (one ion fluoresces), and 85.2% of the cases are detected correctly when both ions are in $|\uparrow\rangle$ (both ions fluoresce). These detection probabilities are independent of the number of repetitions and reduce the visibility of the parity by approximately 14%. In future experiments, the photo detection will be improved by measuring the final state using a fast, spatially resolving detector.

* wunderlich@physik.uni-siegen.de

[1] S. Meiboom and D. Gill, Modified Spin-Echo Method for Measuring Nuclear Relaxation Times. Rev. Sci. Instrum. **29,** 688 (1958).

[2] N. Timoney *et al.*, Quantum Gates and Memory using Microwave Dressed States. Nature **476,** 185 (2011).

[3] D. F. V. James, Quantum dynamics of cold trapped ions with application to quantum computation. Appl. Phys. B **66,** 181 (1998).